ELSEVIER

Contents lists available at ScienceDirect

Journal of Building Engineering

journal homepage: www.elsevier.com/locate/jobe



Waste eggshell valorization in the production of bricks: impact of its addition in different grain-sizes on their mineralogy, physical properties and durability

G. Cultrone ^{a,*}, L. Crespo-López ^{a,b}, R. Jiménez Doblas ^a, M. López Gómez ^a

ARTICLE INFO

Keywords: Eggshell Firing temperature Mineralogical changes Compactness Durability

ABSTRACT

World egg production currently exceeds 97 million tonnes, and if not correctly disposed of, waste eggshell can pose a potential public health risk. Although eggshell has applications in the cosmetic and pharmaceutical industry, less is known about its reuse in the construction sector, with most research focusing on the production of cementitious materials due to its high calcium content. Very little work has been done on its possible use in brick manufacture. In this study, solid brick samples were produced, either without additives or with the addition of 20 % by weight of eggshell with two different grain sizes, fine and coarse. Samples were fired at 800, 950 and 1100 °C. The addition of eggshell results in the formation of gehlenite at 1100 °C in the bricks with coarse residue, and anorthite and wollastonite in those with fine residue. The samples made with coarse residue showed levels of portlandite due to the hydration of CaO. The water absorption capacity was higher in the bricks that contained eggshell, especially coarse-grained, and decreased as the firing temperature increased due to the vitrification of the clay matrix. Vitrification also caused an increase in pore size. The samples without additives and those with fine eggshell were the most compact. The bricks containing coarse eggshell had larger pores, which together with the formation of portlandite reduced their compactness. Finally, the resistance of the bricks to salt crystallization improved as the firing temperature increased, especially at 1100 °C. At this temperature, the most durable bricks were those without residues, although those fired with fine eggshells showed very similar values. At lower firing temperatures, there was greater variability in the results although, in general, the bricks with eggshell seem to resist better than those without it. This work has shown that eggshell, especially fine-grain, could be a valuable resource for the production of efficient and durable bricks.

1. Introduction

Bricks have been a common construction material throughout human history and are still used all over the world today. The manufacturing process has remained unchanged over the centuries and bricks remain one of the most in-demand materials in the construction sector. However, brick production relies heavily on clay, a non-renewable natural resource, often to the point of over-exploitation. This can have significant environmental impacts from damaging fertile topsoil to environmental pollution [1].

E-mail address: cultrone@ugr.es (G. Cultrone).

^a Department of Mineralogy and Petrology, Faculty of Sciences, University of Granada, Spain

^b Scientific Instrumentation Center, University of Granada, Spain

^{*} Corresponding author.

Worldwide brick production is around 1.5 trillion units, and the biggest producer is China, followed by India and Pakistan [2]. The use of bricks in the building industry generates a huge amount of construction and demolition waste (around one billion tonnes/year in China alone). As a result, the Chinese and other governments are implementing policies to increase the use of recycled materials in construction projects [3]. This concern has also extended to the scientific field, where research has been conducted into the reuse of waste from quarrying and building demolition, including old bricks, in the manufacture of new bricks [4–6]. In this sense, bricks are quite versatile in that many different types of residues can be mixed with clay as additives in brick production. Several review papers have explored a wide range of possible residues that can be used as additives, and the benefits and drawbacks of their use [7–9]. It has been found for example that organic additives such as tea waste, coffee grounds and sawdust can increase the porosity of bricks and thus improve their thermal insulation [10–12], while inorganic additives such as household glass increase their compactness and mechanical strength [13].

Among possible organic additives, eggshell is a bio-waste which is classified by the European Commission as a hazardous material mainly because of its organic content, which attracts rats and other organisms, making it a potential public health problem [14]. According to the Food and Agriculture Organisation of the United Nations, world egg production exceeded 97 million tonnes in 2023 (latest data available). Such a large egg production inevitably leads to eggshells from households and the catering industry accumulating in landfills. However, some eggshell is recycled thus promoting a range of sustainable initiatives [15]. For example, it has important applications in the pharmaceutical and cosmetics fields, and is also used as a catalyst and in fertiliser [16-19]. In the construction sector, eggshell has been tested with some success in the manufacture of cementitious materials. Several review papers have analysed the advantages of its use as an additive and the factors that most influence the performance in concretes [20–24]. As for bricks, very little research has been done on the addition of eggshell. In some research studies, calcined eggshell was mixed with other wastes, such as ground granite or rice husk, together with clay to manufacture bricks [25,26]. In one case, instead of using clay, the researchers used a zeolite-poor rock mixed with eggshell to make the bricks [27]. In these papers, the influence of eggshell on the quality of the bricks is partially masked by the presence of other additives. In those research papers in which eggshell alone was used as an additive to mix with the clay, the best physical-mechanical results were obtained with the highest percentage of added eggshell, regardless of whether the samples were fired at 1000 °C (with 10 % of eggshell, [28]) or 1100 °C (with 20 % of eggshell, [29]). It seems that Tangboriboon et al. [28] also tested bricks with eggshell fired at 800, 900 and 1100 °C, but did not present the results obtained at those temperatures. So far, no comparisons have been made between bricks containing eggshell fired at different temperatures, a key factor in the physical-mechanical behaviour of the bricks, and no work has been done to verify the extent to which eggshell granulometry affects the durability of the bricks. The aim of this paper is to investigate in-depth the possibility of recycling eggshells in the manufacture of bricks fired at 800, 950 and 1100 °C. The use of this waste material would, firstly, guarantee a reduction in the demand for clay, a limited natural resource, and, secondly, promote an alternative way of reusing an organic residue that would otherwise end up in landfills. Unlike in the previous studies referred to above, in this study the eggshells were not calcined before being added to the raw material, as they will undergo calcination anyway during the firing of the bricks. The idea is to avoid increasing the cost of brick production due to additional, possibly unnecessary treatments of the residue. For this reason, in this research the use of crushed eggshells (coarse residue) was compared with that of finely ground eggshells. In the former, the eggshells do not have to be ground in a mill, so saving time and energy in the preparation process. Finally, it was decided not to wash the eggshells with tap water before grinding so as to avoid additional water consumption.

As mentioned above, eggshells are an important source of calcium carbonate, a compound that has been shown to act as a low-temperature fluxing agent and is involved in the mineralogical reactions of the bricks [30,31]. To analyse the effect of this phase on the performance of the bricks, carbonate-free clay soil was deliberately chosen as the main raw material. This will facilitate the comprehension of which changes in the mineralogy and physical properties of the bricks are due to the addition of this residue.

2. Materials and methods

The raw material used to make the bricks was collected in the Serranía de Cuenca $(40^{\circ}07'11.6''N)$ and $1^{\circ}09'59.2''W)$, about 50 km from Teruel (Spain). The area is characterised by a substrate dominated by Mesozoic sedimentary rocks, mainly limestones, dolomites and marls formed in shallow marine environments during the Jurassic and Cretaceous era, with a marked influence of the Alpine orogeny that folded these materials [32]. The clays used in this research to make the bricks belong to the Villar del Arzobispo Formation and are fine sediments with a distinctive red colour, which were deposited on marine platforms and coastal lagoons during the Middle-Upper Jurassic, associated with marly strata intercalated with gypsum layers and calcarenites [33,34].

The eggshells used in this study were collected over the course of approximately three months after household consumption. Once the desired amount had been collected to make the bricks, the eggshells were dried and crushed. Two particle sizes, fine and coarse, were produced. The fine fraction was obtained by mechanical pulverisation using a Fritsch Pulverisette 23 ball mill. The coarse fraction was crushed by hand using an agate mortar. The bricks with and without eggshell were manufactured by hand. The clay soil was first sieved to remove fragments of over 2 mm and then dry-mixed with 20 % by weight of either fine or coarse eggshells. This percentage of eggshell was selected on the basis of the limited available literature in which it was found that 20 % eggshell is ideal for improving certain physical-mechanical properties of the bricks [27,28] and given that using the highest feasible percentage is one of the objectives of recycling waste materials [35].

A group of samples without additives was prepared as a control. Tap water was gradually added to knead the clay to the desired consistency. The mass was then placed in a wet wooden mould measuring $12 \times 16 \times 4$ cm and compacted by pressing it with the palm of the hand. When the mould was filled, the top of the mass was smoothed with a ruler to obtain a flat surface. After 24 h, the raw bricks were unmoulded and cut into 4 cm cubes with a stretched cotton thread. The samples were left to dry for a week. The bricks were then

fired in a Herotec CR-35 electric oven under oxidizing conditions at 800, 950 and 1100 °C to study the effect of this temperature range on the mineralogy, texture and physical properties of the bricks. The temperature of the oven was increased at a rate of 5 °C/min. Once the maximum temperature was reached, it was maintained for 3 h, after which the oven was switched off. The samples were left in the oven until the next day to allow them to cool slowly and so avoid cracking due to the β -to- α quartz phase transition at 573 °C [36]. After being taken out of the oven, the bricks were immersed in water for half an hour to prevent "lime blowing" [37], a phenomenon which could occur in the samples with added eggshell. The types of bricks studied in this paper is listed in Table 1.

The granulometry of the clayey material and the fine eggshell was measured with a laser beam in the range $0.02\,\mu\text{m}-1.5\,\text{mm}$ using a Malvern Instruments Mastersizer 2000 apparatus.

The chemical composition of the clayey material was determined by X-ray fluorescence (XRF) using a PANalytical Zetium compact spectrometer with a Rh anode and a 4 kV X-ray generator.

The mineralogy of the clayey material, eggshell and fired bricks was determined by X-ray diffraction (XRD) following the disorder powder method. A PANalytical X'Pert Pro diffractometer was used with the following working conditions: CuK α radiation (λ = 1.5405 Å), 45 kV, 45 mA, 3–70° 20 explored area and 0.01 20/s goniometer speed. HighScore software v.4.8 (Malvern Panalytical) was used to identify the mineral phases by comparing the experimental diffraction patterns with those in the International Centre for Diffraction Data.

The mineralogy and texture of the bricks were observed under a Carl Zeiss Jenapol-U polarized optical microscope (POM) coupled with a Nikon D7000 digital camera.

Hydric tests were carried out to investigate the ability of bricks to absorb water and dry out. Free (A_b) and forced water absorption (A_f) , and drying tests were carried out according to UNE-EN 13755 [38] and NORMAL 29/88 [39] standards. The degree of pore interconnection (Ax) was determined following Cultrone et al. [40], while the saturation coefficient (S), open porosity (P_o) , and apparent (ρ_a) and real densities (ρ_r) were calculated according to the RILEM TC25-PEM [41] standard. Three samples per brick type were analysed under controlled thermo-hydrometric conditions $(20\,^{\circ}\text{C})$ and 30 % relative humidity).

The study of the pore system of bricks was completed by determining the pore size distribution by mercury injection porosimetry (MIP) using a Micromeritics Autopore V 9600 porosimeter. One fragment of about 1 g per brick type was analysed. Specific surface area (SSA), open porosity (P_{OMIP}), and apparent (P_{OMIP}) and real densities (P_{OMIP}) were also determined.

The compactness of the bricks was measured using a Panametrics HV Pulser/Receiver 5058 PR ultrasound apparatus with transducers of 1 MHz and a contact surface of 3 cm in diameter coupled with a Tektronix TDS 3012B oscilloscope. The propagation of P-waves was measured in the three perpendicular directions of the dry cubic samples following the ASTM D2845 [42] standard. The anisotropy (ΔM) was calculated as follows:

$$\Delta M = rac{V_{max} - V_{min}}{V_{max}} imes 100$$

where V_{max} and V_{min} are the maximum and minimum P-wave velocities in the bricks regardless of the measurement direction.

A Konica Minolta CM-700d portable spectrophotometer was used to measure the colour of the bricks in accordance with the UNE-EN 15886 [43] standard. A CIE illuminant D65 was chosen to measure the lightness (L*), chromatic coordinates (a* and b*), chroma (C*) and hue angle (h $^{\circ}$). A pulsed xenon lamp illuminated an 8 mm diameter circular area of the bricks. Four measurements were made per each type of brick. The colour difference in the bricks (Δ E) due to the addition of eggshell was calculated as follows:

$$\Delta \mathbf{E} = \sqrt{\left(\Delta L^*\right)^2 + \left(\Delta a^*\right)^2 + \left(\Delta b^*\right)^2}$$

where ΔL^* , Δa^* and Δb^* are the differences between the lightness and chromaticity values of the bricks made without additives and those made with added eggshell.

Finally, 15 salt crystallization cycles were performed to assess the durability of bricks against salt attack. The test was carried out according to the UNE-EN 12370 [44] standard. The edges of the samples were marked in black before testing. The damage produced by cyclic dissolution and precipitation of $Na_2SO_4 \times 10H_2O$ in the pores and fissures of the bricks was evaluated daily by visual inspection and weight measurement.

3. Results and discussion

3.1. Composition of the clayey material and eggshell

The clay soil from Teruel (T0) has a particle size distribution of between 0.2 and 100 μ m with a maximum at 10 μ m. The curve for the fine eggshell fraction is slightly to the right of the curve for the clay soil, with a maximum at 30 μ m and a wider range of particle

Table 1
Acronym of bricks studied based on the percentage by weight of eggshell and the firing temperatures.

Eggshell	800 °C	950 °C	1100 °C
0 %	T0-800	T0-950	T0-1100
20 % fine	T20F-800	T20F-950	T20F-1100
20 % coarse	T20G-800	T20G-950	T20G-1100

sizes between 0.2 and 800 μ m (Fig. 1). The coarse eggshell fraction could not be analysed using this technique because its particle size exceeded the instrument's measurement range. These fragments do not exceed 5 mm in size, and most are about 2–3 mm to the naked eye.

The chemistry of the clayey raw material shows that it is very rich in silica and has a high alumina content (Table 2). This suggests the presence of quartz, phyllosilicates and/or feldspars. An iron content of over 8 % suggests the presence of Fe compounds. Given the very low MgO and CaO content, the raw material from Teruel can be considered free of carbonates. A K content of nearly 4 % could be related to phyllosilicates and feldspars. Finally, a loss on ignition (LOI) of almost 6 % is due to possible decomposition of organic matter and dihydroxylation of phyllosilicates.

Mineralogically, the raw material from Teruel is rich in quartz and phyllosilicates (Fig. 2). The latter are composed of muscovite and kaolinite. Other phases detected were microcline and hematite. The presence of this oxide, even in trace amounts, explains the red colour of the raw material. The eggshell is composed exclusively of calcite (Table 3).

3.2. Mineralogy of the fired bricks

In the bricks without additives fired at 800 °C, kaolinite was no longer identified. In fact, this phyllosilicate decomposes between 440 and 530 °C, depending on the heating rate [46]. The other phyllosilicate, illite/muscovite, maintains about the same concentration but loses the OH⁻ hydroxyls at around 600 °C [47]. Its amount decreases significantly at 950 °C and it is no longer detected at 1100 °C (Table 3). According to Rodriguez Navarro et al. [48], this phase is epitaxially replaced by mullite. Indeed, the diffractograms show trace amounts of this nesosilicate at 950 °C and increases in concentration at 1100 °C. Another phase that undergoes change as firing temperature increases is the K-feldspar. Identified as microcline in the raw material, it becomes orthoclase at 800 and 950 °C and sanidine at 1100 °C, the most stable high-temperature phase. Quartz is the most abundant mineral and remains almost constant up to 1000 °C, after which its concentration decreases slightly as it participates in reactions to form new silicates [49]. Finally, the amount of hematite increases in line with increasing temperature. This is because the amorphous iron contained in the raw material is converted into hematite, as happens with that present in the lattice of the phyllosilicates [50].

The addition of eggshell induces changes in the mineralogy of the bricks due to the calcitic composition of the additive. This carbonate is still detectable in the bricks fired at 800 and 950 °C, but is no longer present at 1100 °C (Table 3). According to Rodriguez Navarro et al. [51], calcite starts to decompose into CaO at 600 °C and the process is completed at 850 °C. However, the relatively short firing time of the bricks and the significant presence of calcite from the eggshell, which increases the partial pressure of CO₂ in the oven, causes a delay in the decomposition of this carbonate [52,53]. Depending on the granulometry of the eggshell, fine or coarse, other minerals can be identified. One of them, portlandite, is detected in the bricks with coarse residue at all three firing temperatures. The presence of eggshell fragments with sizes up to 5 mm hindered the complete reaction of the CaO (which itself was formed by calcination of the calcite during the firing process) with the silicates in the matrix. The unreacted CaO is hydrated to form portlandite (Ca(OH)₂). The other phases identified are gehlenite, anorthite and wollastonite, which are Ca-silicates that only appear at 1100 °C (Table 3). Interestingly, these three phases do not form in both types of brick. Anorthite and wollastonite are present in the fine-eggshell bricks, while gehlenite is only detected in the coarse-eggshell bricks. Considering that the formation of these new phases is controlled by reaction-diffusion processes [30], it seems likely that the presence of finer calcite particles spread and accelerated these reactions to allow the crystallization of anorthite and wollastonite, as compared to bricks with coarse residue where gehlenite was the only phase detected. According to Cultrone and Carrillo Rosua [47] and Traoré et al. [54], anorthite and wollastonite should form after gehlenite. We assume that in T20F-1100 gehlenite may have formed below 1100 °C and was replaced by the other two silicates at 1100 °C according to the following reaction:

Quartz Gehlenite Anorthite Wollastonite

 $2SiO_2 + Ca_2Al_2SiO_7 \rightarrow CaAl_2Si_2O_8 + CaSiO_3$

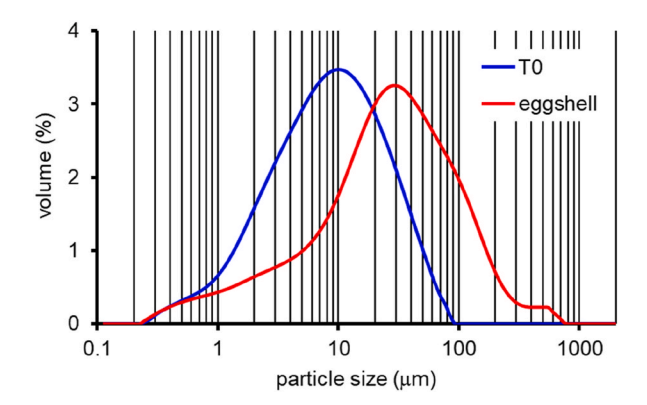


Fig. 1. Grain size distribution curves for the raw material from Teruel (T0) and the fine eggshell residue.

Table 2Mayor elements (in wt.%) of the raw material from Teruel (T0).

	SiO ₂	Al ₂ O ₃	Fe ₂ O ₃	MnO	MgO	CaO	Na ₂ O	K ₂ O	TiO ₂	P_2O_5	LOI	tot
T0	59.25	19.77	8.67	0.04	1.13	0.34	0.19	3.85	0.81	0.11	5.83	99.99

LOI = loss on ignition.

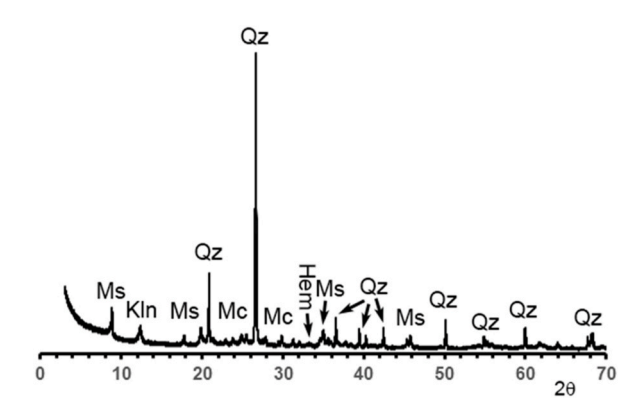


Fig. 2. X-ray diffraction pattern of the clayey material from Teruel. Qz = quartz; Ms = muscovite; Kln = kaolinite; Mc = microcline; Hem = hematite. Mineral abbreviations after Warr [45].

Table 3Mineralogy of eggshell, unfired and fired bricks.

,	Qz	Ms	Kln	Hem	Mc	Or	Sa	Cal	Prt	Mul	Gh	An	Wo
Eggshell								xxx					
T0	XXX	xx	x	tr	x								
T0-800	XXX	XX		x		x							
T0-950	XXX	tr		x		x				tr			
T0-1100	xx			xx			x			x			
T20F-800	XXX	XX		x		x		X					
T20F-950	XXX	x		x		x		X		tr			
T20F-1100	xx			XX						x		x	tr
T20G-800	xxx	XX		x		x		x	tr				
T20G-950	xxx	x		x		tr		x	tr				
T20G-1100	xx			xx			tr		x	tr	tr		

xxx = abundant; xx = frequent; x = scarce; tr = in traces; Qz = quartz; Ms = muscovite; Kln = kaolinite; Hem = hematite; Mc = microcline; Or = orthoclase; Sa = sanidine; Cal = calcite; Prt = portlandite; Mul = mullite; Gh = gehlenite; An = anorthite; Wo = wollastonite. Mineral abbreviations after Warr [45] and Whitney and Evans [55].

As regards the amount of new calcium silicates formed at $1100\,^{\circ}$ C in the bricks made with eggshell, it was found that smaller amounts of silicates were formed in T20G-1100 than in T20F-1100. This result is logical, given that in the fine-residue bricks all the available calcite reacts and converts to anorthite (plus traces of wollastonite), whereas in the coarse-residue bricks some of the calcite is converted into portlandite, so reducing the calcite-silicate reaction, leaving only traces of gehlenite (Table 3).

3.3. Texture of the bricks

The observation under the microscope of the bricks made without additives shows that at 800 °C (T0-800) they have a compact, uniform, red-coloured matrix in which grains of gneiss up to 1 mm can be seen (Fig. 3a). They also contain isolated quartz fragments with angular morphology and undulose extinction. Small muscovite-type phyllosilicates are dispersed in the matrix. Some of the muscovite crystals reach the blue-green second-order interference colour. Rare opaque grains can also be seen. Pores are rounded to elongated in shape. At 950 °C, the texture appears similar to that of the bricks fired at 800 °C. The only difference is that the matrix tends to be slightly darker and more compact, indicating that sintering has taken place between the particles [56]. At 1100 °C, the matrix becomes dark due to extensive vitrification and only quartz grains can be distinguished, together with a few phyllosilicates which have lost their birefringence and turned white (Fig. 3b). According to the XRD results, they could correspond to mullite that has replaced the muscovite. The pores appear to be more rounded.

The addition of eggshell results in some changes in the texture of the samples. In the case of the fine residue (T20F samples), small eggshell grains of calcitic composition, partially decomposed by firing, are observed (Fig. 3c). At 800 °C, these grains are uniformly

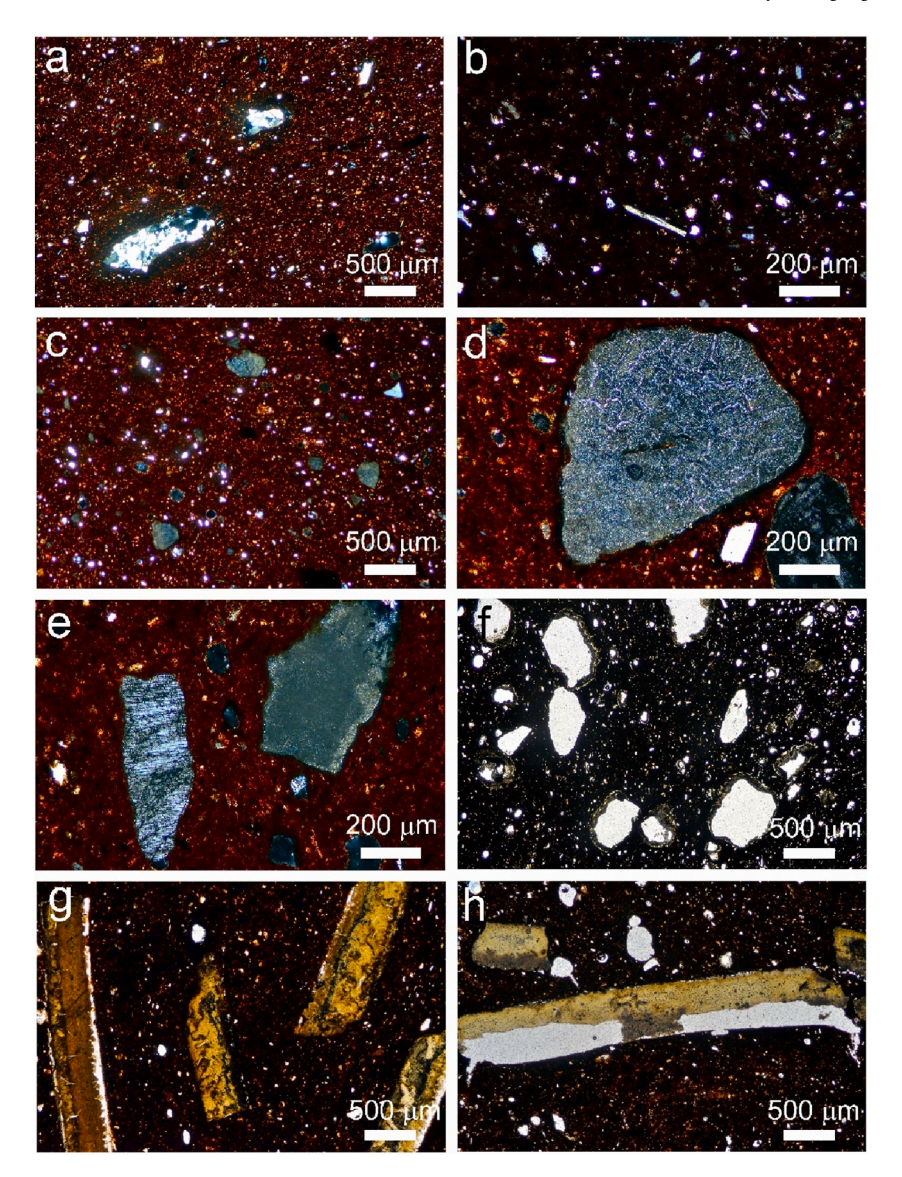


Fig. 3. Optical microscope images of bricks made with and without eggshell residue. a) general view of T0-800; b) thin muscovite grain of less than 200 μm in length in T0-1100; c) small eggshell grains in T20F-800; d) eggshell fragment in T20F-800 in which there are veins with a high interference colour; e) feldspar and eggshell grains in T20F-950; f) T20F-1100 with the presence of rounded pores, in part due to the loss of eggshell grains; g) T20G-800 showing large, partially fractured eggshell fragments; h) T20G-1100 showing partially detached eggshell grains. Two small fractures are visible at the corners of the elongated pore. Images taken in cross polarized light (a, b, c, d, e) and plane-polarized light (f, g, h).

greyish and small stains and veins can occasionally be observed within them, while preserving the typical birefringence of these carbonates confirming that they are not completely decomposed (Fig. 3d). The presence of eggshells increases the amount of temper in the bricks. This residue is evenly distributed in the matrix together with quartz, phyllosilicates, feldspars (sometimes with perthitic texture, Fig. 3e) and some hematite. As the firing temperature increases, the matrix becomes darker, as happens in the control bricks made without additives. The only difference is an increase in porosity, especially at 1100 °C, because the eggshell fragments have disappeared, leaving empty spaces in their place. Only a few relicts can be observed at the edges of some pores (Fig. 3f).

In T20G samples, large eggshell fragments are visible to the naked eye and appear elongated and curved under the microscope. They are brown to dark grey in colour, sometimes fractured and show few signs of high birefringence at 800 °C. In some cases, there is a separation between the matrix and the eggshell (Fig. 3g). Occasionally, at 950 and 1100 °C the eggshell fragments disappear, leaving elongated pores (Fig. 3h) from which small fractures can branch out. This is linked to the formation of portlandite, previously identified by XRD. The volume of portlandite is greater than that of calcium oxide, causing cracks to develop from the edge of the pores. This is known to cause stresses in materials and could represent a problem for the future strength of the brick [57,58].

3.4. Study of the pore system

Fig. 4 shows the free and forced water absorption and drying curves for the three groups of bricks fired at 800, 950 and 1100 °C. We can see that bricks fired at 800 °C absorb more water than those fired at 950 °C, and the latter are more absorbent than those fired at 1100 °C. However, the differences between 800 and 950 °C are not so pronounced, as the curves are closer to each other than to the 1100 °C curve, where the bricks absorb much less water due to the vitrification of the clay matrix [59]. The results show that in the case of the Teruel clay, vitrification does not occur gradually, but rather in steps, which are much more pronounced in the 950–1100 °C range. The slope of the drying curve for the bricks fired at 1100 °C is quite different from that for the samples fired at the other two temperatures probably because at 1100 °C changes the size of capillaries that control the movement of water to the surface [60]. When comparing the bricks according to their composition, it is evident that the presence of eggshell enhances the capacity to absorb water, and that this capacity is greater in the bricks made with coarse-grain eggshell. The difference is maintained as the bricks dry: in general, the bricks made with coarse eggshell will have a longer drying curve.

Table 4 summarizes the hydric parameters of the bricks. All samples absorb less water as the firing temperature increases, especially at 1100 °C (A_b). The same trend is observed in forced water absorption (i.e., under vacuum, A_f). The capacity to absorb water increases with the addition of eggshell and is higher in the bricks made with the coarse eggshell than in those made with finer eggshell particles. Interestingly, the values for A_b and A_f are quite low when compared to those for other handmade bricks fired at the same temperatures [59,61,62]. If we consider the ISO 13006 [63] standard, which classifies extruded and pressed ceramic tiles on the basis of water absorption, the bricks studied in this paper fall into Group 3 (with A_b over 10 %, samples fired at 800 and 950 °C) and Group 2 (with A_b between 3 and 10 %, samples fired at 1100 °C), the groups for porous earthenware and semi-vitrified red stoneware, respectively. It should be noted that optical microscopy had already revealed that these bricks have a compact texture (Fig. 3), which is responsible for the low absorption parameters. The decrease in the water absorption capacity from 800 to 1100 °C is due to the vitrification of the bricks, which causes a decrease in the interconnection between the pores (Ax augments, Table 4), especially for T0-1100, the brick with the lowest A_b. Ax is inversely related to the saturation coefficient (S): as the pore network becomes more tortuous, the samples saturate less. The tortuosity of the pore system also influences the drying phase (Di), in that the samples with the most tortuous pore systems are the slowest to dry out (higher Di, Table 4). The brick that dries out fastest is T0-800. The open porosity (Po) shows the same trend as water absorption: it decreases as the firing temperature increases and is higher when eggshell is added, above all in the bricks containing coarse fragments. While the samples fired at 800 and 950 °C have similar porosity values, there is a significant decrease at 1100 °C. It is probable that the extensive vitrification of the bricks at this temperature caused coalescence between the small pores, leading to an increased number of larger, closed, or poorly interconnected pores, thereby developing what is known as a "cellular structure" [64]. The real density (ρ_T) ranges from 2.4 to 2.6 g/cm³, which is consistent with the density of quartz and other silicates. The lowest values were recorded at 1100 °C. The complete decomposition at high temperatures of illite/muscovite (see Table 3), the most abundant phase in the clayey raw material along with quartz, and the presence of amorphous (i.e., vitreous) phase may have contributed to this decrease in ρ_r at 1100 °C. The apparent density (ρ_a) shows an opposite trend to the real density, with values of over 2 g/cm³ only at 1100 °C. This is logical given that at this temperature the vitrification of the clay matrix reduces the porosity of the bricks, so creating a denser structure. The values for standard deviation are reasonably low, with a slight increase in line with firing temperature, above all at 1100 °C. This means that the high vitrification of the bricks causes greater variations within their pore system.

In terms of pore size, as measured by MIP, the bricks show a generally unimodal porometric distribution with a maximum peak between 0.1 and 1 μ m (Fig. 5). More specifically, the peak shifted towards larger pore sizes with increasing firing temperature, indicating that the pores were coalescing. As for the height of the peak, it is higher at 950 °C and always lower at 1100 °C. In T0-1100,

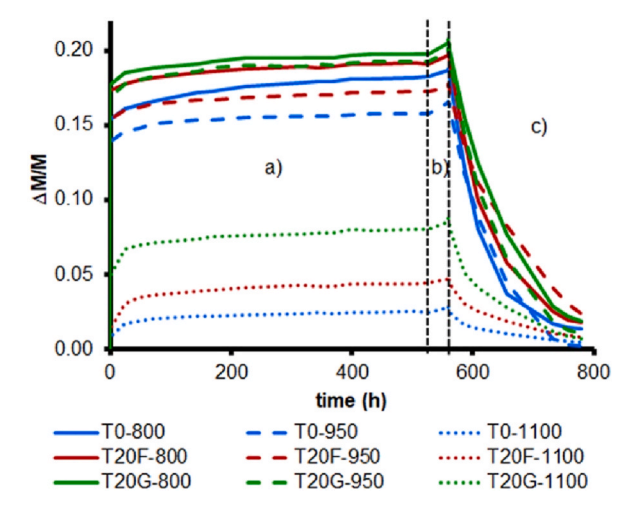


Fig. 4. Free water absorption (a), forced water absorption (b) and drying curves (c) for the studied bricks. Weight variation ($\Delta M/M$) versus time (in hours).

Table 4
Results of hydric and MIP tests on the bricks made without additives (T0) and with added fine (T20F) and coarse 20 wt% eggshell grains (T20C). The standard deviation of each result of the hydric tests is indicated in brackets.

	T0-800	T0-950	T0-1100	T20F-800	T20F-950	T20F-1100	T20C-800	T20C-950	T20C-1100
A _b	18.24	15.79	3.09	19.13	17.30	4.42	19.77	19.26	8.03
	(0.24)	(0.44)	(0.75)	(0.11)	(0.46)	(1.32)	(0.35)	(0.17)	(1.27)
A_f	18.73	16.55	3.40	19.66	17.54	4.69	20.50	19.96	8.52
	(0.24)	(0.57)	(0.80)	(0.18)	(0.46)	(1.32)	(0.50)	(0.17)	(1.48)
Ax	2.63	4.57	9.18	2.69	1.41	5.96	3.57	3.50	5.69
	(0.86)	(0.68)	(0.76)	(0.39)	(0.03)	(1.69)	(0.66)	(0.13)	(1.42)
Di	0.923	0.930	0.964	0.924	0.936	0.960	0.926	0.923	0.948
	(0.002)	(0.004)	(0.000)	(0.002)	(0.002)	(0.004)	(0.004)	(0.005)	(0.004)
S	87.39	89.56	71.39	91.52	92.40	71.93	91.12	90.10	81.16
	(0.97)	(0.57)	(3.05)	(0.99)	(0.28)	(5.82)	(0.78)	(0.64)	(1.25)
P_{o}	32.88	30.38	7.80	33.46	30.86	9.98	34.59	34.16	17.53
	(0.23)	(0.82)	(1.71)	(0.31)	(0.61)	(2.61)	(0.51)	(0.23)	(2.58)
ρ_a	1.75	1.84	2.30	1.70	1.76	2.14	1.69	1.71	2.06
	(0.01)	(0.01)	(0.04)	(0.01)	(0.01)	(0.05)	(0.02)	(0.00)	(0.05)
$\rho_{\rm r}$	2.61	2.64	2.50	2.56	2.54	2.37	2.58	2.60	2.50
	(0.01)	(0.01)	(0.01)	(0.02)	(0.01)	(0.02)	(0.01)	(0.01)	(0.01)
P_{oMIP}	28.74	31.06	6.50	30.55	32.33	18.42	33.19	33.94	15.03
ρ_{aMIP}	1.80	1.81	2.42	1.72	1.80	2.09	1.65	1.72	2.19
ρ_{rMIP}	2.53	2.63	2.59	2.48	2.66	2.56	2.47	2.61	2.59
SSA	6.77	1.82	0.85	6.35	2.00	0.59	6.11	2.34	0.61

 A_b = free water absorption (%); A_f = forced water absorption (%); A_f = degree of pore interconnection; D_f = drying index; S_f = saturation coefficient (%); P_o = open porosity (%); P_o = apparent density (g/cm³); P_o = real density (g/cm³). P_{oMIP} , P_{oMIP} , P_{oMIP} , P_{oMIP} , and SSA are respectively the open porosity (%), apparent density (g/cm³), real density (g/cm³) and specific surface area (m²/g) determined by MIP.

it is so low that the scale of the Y-axis had to be changed to be able to observe the pore families present in this brick. T0-1100 is the only sample with a polymodal pore size distribution, with two main families at 0.1 and 0.72 μ m, and an additional family around 500 μ m (Fig. 5). In any case, it has very low porosity levels, with an open porosity of just 6.5 % (P_{OMIP}, Table 4), a very similar value to that

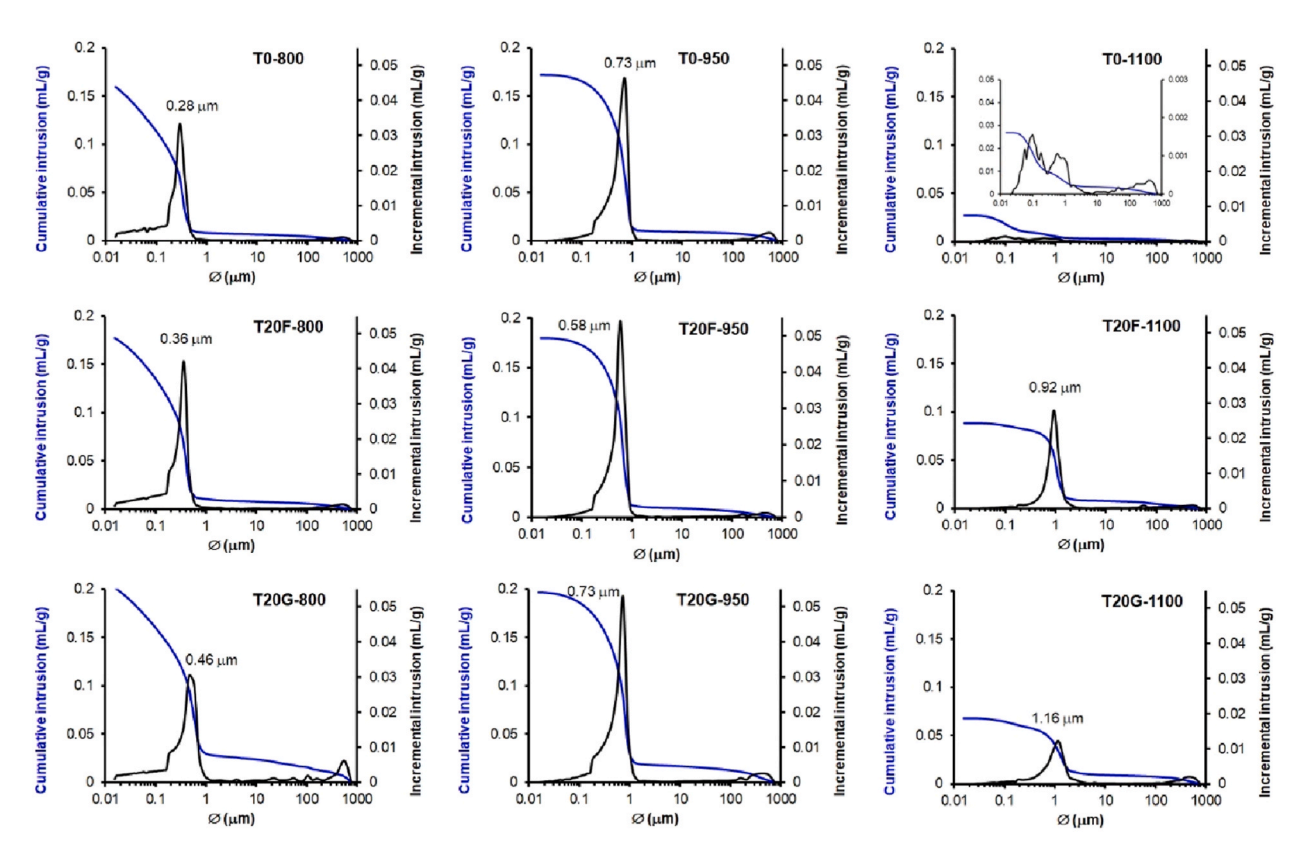


Fig. 5. Pore size distribution (in black) and cumulative mercury intrusion (in blue) curves for the studied bricks. The diameter at the maximum peak in each diagram is indicated.

obtained in the hydric tests. In general, there are no significant differences between the porosity and density values measured by the two techniques. In fact, even with MIP, the porosity is similar between 800 and 950 °C and decreases significantly at 1100 °C, especially in the bricks without additives. The addition of eggshell causes an increase in porosity at all three firing temperatures. It is interesting to note the evolution of the specific surface area (SSA, Table 4), which is similar in the three groups of bricks. The highest SSA values are measured at 800 °C, with values of just over 6 $\rm m^2/g$. In fact, these bricks are the only ones with pores in the 0.01–0.1 $\rm \mu m$ range (Fig. 5). At 950 °C, the SSA is between 1.8 and 2.3 $\rm m^2/g$ and at 1100 °C it goes below 1 $\rm m^2/g$ (Table 4). At 950 °C, although the smallest pores are no longer present, the curves show a certain percentage of pores of between 0.1 and 0.3 $\rm \mu m$, while at 1100 °C they become more symmetrical, at least in the bricks made with additives (Fig. 5). Finally, a separate family of pores was identified at around 500 $\rm \mu m$, something that was more pronounced in the bricks with coarse eggshell (Fig. 5). In a way, the coarse particles are responsible for the increase in this family of pores, maybe linked to the formation of cracks because of portlandite growth.

3.5. Compactness

The propagation velocity of the ultrasonic waves augments as the firing temperature increases, indicating that the bricks become more compact from 800 to 950 °C and even more so at 1100 °C (V_{P^*} , Table 5). V_{P1} is lower than V_{P2} and V_{P3} due to the processing of the samples. V_{P1} is measured according to the direction of compaction of the clay mass, which means that the P-waves propagate perpendicular to the phyllosilicate sheets, so slowing down their transmission inside the bricks. It is noteworthy that the difference between V_{P1} and the other two velocities decreases as firing temperature increases, resulting in a decrease in the anisotropy of the bricks (ΔE , Table 5). This decrease is more pronounced in the bricks fired at 1100 °C, regardless of their composition, because of the high vitrification of the clay mass.

Comparing the three groups of bricks, the highest velocities are measured in the bricks without additives and with fine eggshell grains. It is interesting to note that at 800 and 950 °C, the velocities tend to be slightly higher in the bricks made with additives. The calcite that makes up the eggshell is a low-temperature fluxing agent and favours greater bonding between the brick particles [65], which may promote faster wave propagation. This is not observed in the bricks with coarse eggshell grains, which are more porous, as shown by MIP and hydric tests (see Table 4). The formation of portlandite due to the hydration of calcium oxide only in this group of bricks (see Table 3) has contributed to an increase in the porosity of the samples with the development of cracks, as observed by optical microscopy (see Fig. 3).

3.6. Colour

In terms of colour, the bricks are red like the unfired samples, albeit with a more intense colour. Indeed, when the unfired samples (T0) are compared with the bricks made without additive fired at 800 and 950 °C, the chromatic coordinates (a* and b*) and chroma (C*) are higher in the latter (Table 6). This may be due to the fact that the hematite, the phase responsible for the red colour, was already present in trace amounts in the raw samples and increased in concentration as the bricks were fired (see Table 3). With some exceptions, similar behaviour can be observed in the bricks containing either fine or coarse eggshell residue. The a* and b* values of all the bricks fall within the red-yellow quadrant of the CIEL*a*b* colour space, with little difference between 800 and 950 °C. At 1100 °C there is a clear decrease in both a* and b* due to the high degree of vitrification of the bricks (Table 6). This indicates that it is not the presence or absence of eggshells, but the high temperature (1100 °C) that is responsible for the colour variation. This is reflected in the chroma (C*) value, which is less than 30, and the hue angle (h°), which varies between 41° and 44° only in samples fired at 1100 °C. The lightness varies between 38 and 54, indicating that the bricks tend to be quite dark, especially in the samples fired at 1100 °C (L*, Table 6). The lowest value is measured at T0-1100 and increases after the addition of eggshell, especially in the bricks with the coarse fraction. The presence of white millimetre-sized fragments, easily visible to the naked eye, in all T20G samples is responsible for the higher L* value compared to the other bricks. Interestingly, the eggshell fragments were harder to distinguish in the unfired samples (and the colorimetric values for T20F and T20G are similar to those for T0, Table 6). The highest L* values were always in the bricks fired at 950 °C. This result seems to be related to the sintering of the ceramics at this temperature as described earlier (see "Texture of

Table 5Compactness of the bricks without and with added eggshell.

	V_{P1}	V_{P2}	V_{P3}	$\overline{V_P}$	ΔM
T0-800	1131	1697	1488	1439	33.3
T0-950	2129	2195	2368	2231	10.1
T0-1100	3774	4032	3855	3887	6.9
T20F-800	1343	1624	1654	1540	18.8
T20F-950	1967	2411	2393	2257	18.4
T20F-1100	3716	3989	3750	3819	6.9
T20G-800	1080	1461	1374	1305	26.1
T20G-950	1634	2013	2102	1916	22.3
T20G-1100	2906	3100	3097	3034	6.3

 V_{P1} , V_{P2} and V_{P3} = velocities of the P waves (m/s) along the three orthogonal directions of the brick cubes; $\overline{V_P}$ = mean wave velocity (m/s); ΔM = anisotropy (%).

Table 6
Colour of the unfired and fired bricks without and with added eggshell. Each value is the mean of four measurements. The standard deviation appears in brackets.

	L*	a*	b*	C*	h°
T0	47.69 (1.16)	24.13 (0.23)	16.68 (0.67)	35.97 (0.63)	47.87 (0.52)
T20F	47.69 (0.49)	23.81 (0.43)	25.98 (0.45)	35.25 (0.61)	47.50 (0.10)
T20G	46.96 (1.09)	23.21 (1.26)	25.66 (1.60)	34.60 (2.03)	47.85 (0.34)
T0-800	48.87 (0.40)	27.48 (0.19)	29.37 (0.23)	40.23 (0.29)	46.91 (0.10)
T0-950	50.73 (0.35)	27.66 (0.32)	31.80 (0.56)	42.15 (0.63)	48.98 (0.17)
T0-1100	38.35 (0.06)	18.98 (0.32)	17.21 (0.38)	25.62 (0.46)	42.21 (0.38)
T20F-800	46.33 (0.36)	28.81 (0.15)	30.06 (0.39)	41.64 (0.39)	46.21 (0.24)
T20F-950	52.98 (0.50)	25.43 (0.18)	28.13 (0.24)	37.92 (0.26)	47.89 (0.21)
T20F-1100	41.64 (2.41)	15.47 (1.58)	13.72 (1.71)	20.68 (2.31)	41.50 (0.70)
T20G-800	50.78 (1.39)	25.71 (0.89)	27.28 (1.13)	37.48 (1.40)	46.69 (0.51)
T20G-950	54.16 (0.68)	25.36 (1.25)	28.07 (2.68)	37.84 (2.82)	47.83 (1.39)
T20G-1100	47.44 (5.44)	21.08 (3.57)	20.38 (5.55)	29.35 (6.44)	43.63 (2.70)

 $L^* = lightness$; a^* and $b^* = chromatic coordinates; <math>C^* = chroma$; $h^\circ = hue$ angle.

bricks" section). Sintering would probably have reduced the surface roughness of the samples, so increasing the lightness, but without reaching the extensive degree of vitrification noted at $1100\,^{\circ}$ C, which was accompanied by a darkening of the samples (i.e., a decrease in the L* values).

3.7. Durability

A quick look at Fig. 6 shows how the resistance of the bricks against salt attack is affected by the firing temperature. Indeed, all the bricks fired at 800 °C (continuous lines) suffer significant weight loss at the end of the test. More specifically, these samples show an increase in weight during the first 4-7 test cycles due to the crystallization of salts in the porous system. After that, the bricks begin losing very small fragments (i.e. powdering, according to ICOMOS-ISCS [66]), first at the corners and edges of the cubes and then on the faces. By the end of the test, these samples have acquired a rounded shape (Fig. 7). TO-800 is the brick that started to break first (3rd cycle) and behaved worst at the end of the test. At 950 °C the samples are subject to great variations in weight and appear partially deteriorated, mainly at the edges (Fig. 7). This is due to the sintering process between the particles, which prevents the bricks from powdering, but is not enough to prevent them from losing larger fragments than the samples fired at 800 °C (fragmentation, according to ICOMOS-ISCS [66]). This is particularly evident in T20F-950 as compared to the other two samples fired at the same temperature (Fig. 6). This brick shows an initial increase in weight up to the third cycle, which from then on increases more quickly up to the seventh cycle due to the crystallization of the sodium sulphate in the pore system. In the next cycle, number eight, there is a loss of weight due to the pressure exerted by the salts in confined spaces, which causes fissures to develop and fragments to be lost. The weight increases again in the ninth cycle due to the precipitation of salts in the new pores and fissures created in the brick. After this, there is a succession of weight losses and gains, creating a sawtooth-shaped curve. At 1100 °C, the samples show only a very slight but steady increase in weight over the test's 15 cycles (Fig. 6) and appear intact to the naked eye. The edges marked in black are still perfectly visible (Fig. 7). When comparing the samples made with and without additives, two trends can be observed. At 800 and 950 °C, the samples with the greatest weight loss are those without additives. This confirms the ultrasound data and, as mentioned earlier, may be because calcite acts as a melting agent at low firing temperatures. This creates a greater degree of bonding between the particles compared to the bricks without eggshell. At higher temperatures (1100 °C), it is the extensive vitrification that ensures the strength of the bricks and prevents damage due to salt crystallization. The bricks made without additives are more resistant to salt attack (Fig. 6). This is because new pores appear at 1100 °C in spaces that were previously filled by eggshell grains (see Po values at 1100 °C, Table 4). Sodium sulphate crystallizes in these new pores, potentially causing fissures to appear. When these bricks are compared with others fired at similar temperatures, the beneficial effect of the carbonate present in the eggshell becomes noticeable at low firing temperatures. While the bricks are all highly resistant at 1100 °C due to the vitrification of the clay matrix, it is clear at lower temperatures that the melting action of the carbonates improves durability compared to bricks containing other organic [67,68] and inorganic additives [69].

4. Summary and conclusions

In this paper, the effects of adding fine and coarse eggshell on the production of bricks by using a carbonate-free raw material was investigated. The following has been determined.

1) The addition of eggshells to the raw material influences the mineralogy of bricks, resulting in the formation of calcium silicates, phases that are absent in bricks without additives. These calcium silicates vary depending on the grain size of eggshell. Gehlenite is formed in the bricks made with added coarse eggshell while anorthite and wollastonite are formed in those made with fine residue. This is because the formation of calcium silicates is related to reaction-diffusion processes and they occur more quickly when fine eggshell particles are added. The coarse residue is also responsible for the presence of portlandite.

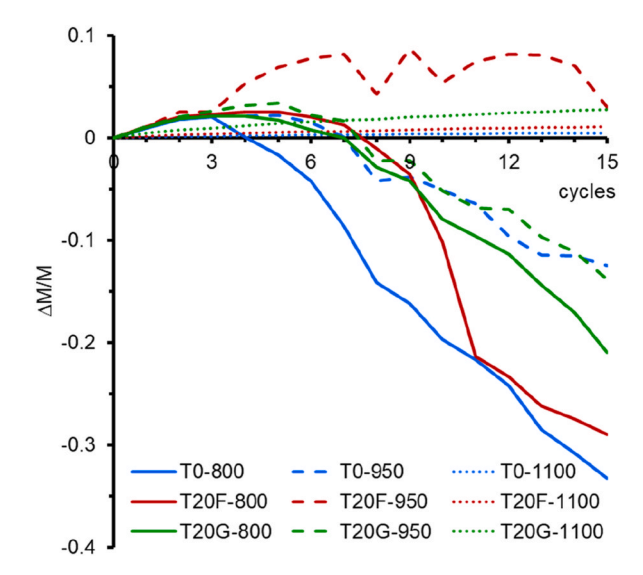


Fig. 6. Salt crystallization test for bricks with and without eggshell. Weight variation ($\Delta M/M$) over the course of the 15 test cycles. Each curve is the mean of three measurements.

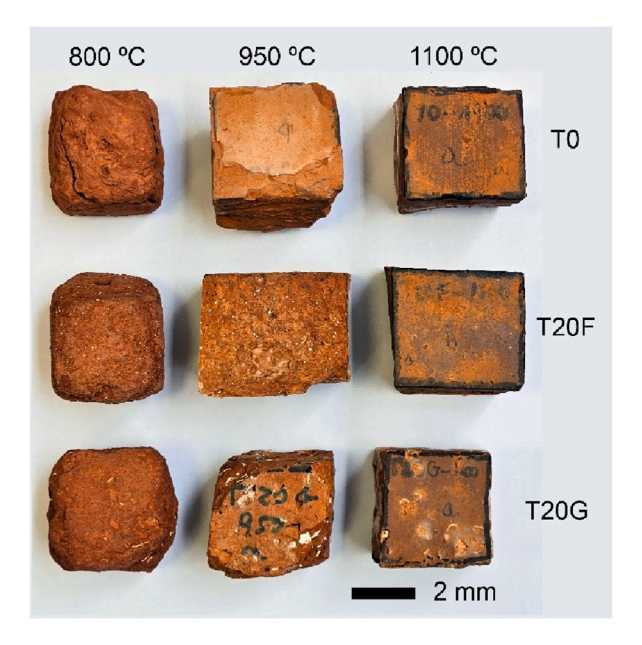


Fig. 7. Visual appearance of the brick samples at the end of the salt crystallization test.

- 2) Texturally, the formation of portlandite promotes the development of fissures in the matrix of bricks fired at 1100 °C because of the hydration of CaO in Ca(OH)₂. Fissures are absent in bricks with fine eggshell were the residue is replaced by pores.
- 3) The pore system of bricks modifies as the firing temperature increases. There is a shift in the largest pore family towards larger pores, the ability to absorb water decreases, and the interconnection between pores also decreases. The samples that retain the least water are those without additives, followed by those with fine eggshell and then those with coarse eggshell. The studied bricks have rather low absorption values compared to the other bricks fired in the same temperature range.
- 4) The increase in firing temperature is accompanied by higher compactness. The least compact bricks were those made with coarse eggshell grains, due to the greater porosity and the development of fissures because of the hydration of CaO in Ca(OH)₂. Therefore, the production of bricks with coarse-grain eggshell may not be advisable.
- 5) The higher the firing temperature, the more durable the bricks are against salt crystallization. Moreover, while at 1100 °C, the most durable bricks were found to be those without additives, at 800 and 950 °C the addition of eggshells makes these bricks more resistant to decay because this additive acts as a fluxing agent at low firing temperatures.

It can be concluded that the low water absorption values measured in the studied bricks make them resistant materials, particularly in environments where the presence of water can cause damage. Furthermore, while high firing temperatures make bricks very durable in environments where soluble salts crystallize, the carbonate of eggshell improves the bond between particles and, in a broader sense, the strength of bricks at lower firing temperatures, ensuring energy and cost savings in brick production. Aesthetically, bricks fired with powdered eggshell show a uniform red colour similar to that of bricks without additives. Therefore, bricks made with this residue can be used in both new buildings and for restoration purposes, where existing pieces need to be replaced with similar-coloured ones. However, the mechanical behaviour of these new bricks must be assessed in order to evaluate their potential for use in construction in accordance with current regulations.

This research has shown how eggshell with a fine grain size could be used as an additive in the manufacture of bricks that are compact and durable, achieving values not dissimilar to those obtained by bricks made without the additive.

CRediT authorship contribution statement

G. Cultrone: Writing – original draft, Supervision, Methodology, Funding acquisition, Conceptualization. **L. Crespo-López:** Supervision, Investigation, Conceptualization. **R. Jiménez Doblas:** Investigation, Formal analysis, Data curation. **M. López Gómez:** Methodology, Investigation, Formal analysis.

Declaration of competing interest

The authors declare that they have no known competing financial interests or personal relationships that could have appeared to influence the work reported in this paper.

Acknowledgements

This research has been financially supported by the RNM179 research group of the Junta de Andalucía and the research project PID2023-146405OB-100 (2024–2027, funded by MICIU/AEI/10.13039/501100011033 and FEDER, UE). Funding for open access charge: Universidad de Granada/CBUA. We are grateful to Nigel Walkington for his assistance in revising the English version of the manuscript. We would like to thank to anonymous referees for their in-depth reviews.

Data availability

Data will be made available on request.

References

- [1] A.B. Madavi, Environmental impact of bricks making process in Umbraj and Masur area, in: M.M. Barwant, V.K. Manam (Eds.), Environment Conservation, Challenges Threats in Conservation of Biodiversity (Volume III), Scieng Publications, 2022, pp. 196–202.
- [2] CCAC, Mitigating black carbon and other pollutants from brick production, Awareness materials, www.ccacoalition.org/, 2015.
- [3] M.R. Maaze, S. Shrivastava, Development and performance evaluation of recycled brick waste-based geopolymer brick for improved physico-mechanical, brick-bond and durability properties, J. Build. Eng. 97 (2024) 110701, https://doi.org/10.1016/j.jobe.2024.110701.
- [4] J. Rukijkanpanich, N. Thongchai, Burned brick production from residues of quarrying process in Thailand, J. Build. Eng. 25 (2019) 100811, https://doi.org/ 10.1016/j.jobe.2019.100811.
- [5] C. Zanelli, E. Marrocchino, G. Guarini, A. Toffano, C. Vaccaro, M. Dondi, Recycling construction and demolition residues in clay bricks, Appl. Sci. 11 (2021) 8918, https://doi.org/10.3390/app11198918.
- [6] M. Dubale, M.V. Vasić, G. Goel, A. Kalamdhad, B. Laishram, The recycling of demolition roof tile waste as a resource in the manufacturing of solid bricks: a scale-up to the industry, Constr. Build. Mater. 412 (2024) 134727, https://doi.org/10.1016/j.conbuildmat.2023.134727.
- [7] L. Zhang, Production of bricks from waste materials a review, Constr. Build. Mater. 47 (2013) 643-655, https://doi.org/10.1016/j.conbuildmat.2013.05.043.
- [8] P. Muñoz, M.P. Morales, V. Letelier, M.A. Mendívil, Fired clay bricks made by adding wastes: assessment of the impact on physical, mechanical and thermal properties, Constr. Build. Mater. 125 (2016) 241–252, https://doi.org/10.1016/j.conbuildmat.2016.0.024.
- [9] C. Dhanjode, A. Nag, Utilization of landfill waste in brick manufacturing: a review, Mater. Today Proc. 62 (2022) 6628–6633, https://doi.org/10.1016/j. matpr.2022.04.616.
- [10] S. Ozturk, M. Sutcu, E. Erdogmus, O. Gencel, Influence of tea waste concentration in the physical, mechanical and thermal properties of brick clay mixtures, Constr. Build. Mater. 217 (2019) 592–599, https://doi.org/10.1016/j.conbuildmat.2019.05.114.
- [11] G. Cultrone, I. Aurrekoetxea, C. Casado, A. Arizzi, Sawdust recycling in the production of lightweight bricks: how the amount of additive and the firing temperature influence the physical properties of the bricks, Constr. Build. Mater. 235 (2020) 117436, https://doi.org/10.1016/j.conbuildmat.2019.117436
- [12] R. Ordieres, G. Cultrone, Technical quality of solid bricks made using clayey earth with added coffee grounds and fly ash, Constr. Build. Mater. 341 (2022) 127757, https://doi.org/10.1016/j.conbuildmat.2022.127757.
- [13] L. Crespo López, G. Cultrone, Improvement in the physical properties of solid bricks by adding household glass waste, J. Build. Eng. 59 (2022) 105039, https://doi.org/10.1016/j.jobe.2022.105039.
- [14] S. Mignardi, L. Archilletti, L. Medeghini, C. De Vito, Valorization of eggshell biowaste for sustainable environmental remediation, Sci. Rep. 10 (2020) 2436, https://doi.org/10.1038/s41598-020-59324-5.
- [15] M.J. Quina, M.A.R. Soares, R. Quinta Ferreira, Applications of industrial eggshell as a valuable anthropogenic resource, Resour. Conserv. Recycl. 123 (2017) 176–186, https://doi.org/10.1016/j.resconrec.2016.09.027.
- [16] A.M. King'ori, A review of the uses of poultry eggshells and shell membranes, Int. J. Poultry Sci. 10 (2011) 908–912.
- [17] A. Laca, A. Laca, M. Díaz, Eggshell waste as catalyst: a review, J. Environ. Manag. 197 (2017) 351–359, https://doi.org/10.1016/j.jenvman.2017.03.088.
- [18] T.A.E. Ahmed, L. Wu, M. Younes, M. Hincke, Biotechnological applications of eggshell: recent advances, Front. Bioeng. Biotechnol. 9 (2021) 675634, https://doi.org/10.3389/fbioe.2021.675364.
- [19] L. Iftikhar, I. Ahmad, M. Saleem, A. Rasheed, A. Waseem, Exploring the chemistry of waste eggshells and its diverse applications, Waste Manage. (Tucson, Ariz.) 189 (2024) 348–363, https://doi.org/10.1016/j.wasman.2024.08.024.

- [20] D. Yang, J. Zhao, W. Ahmad, M.N. Amin, F. Aslam, K. Khan, A. Ahmad, Potential use of waste eggshells in cement-based materials: a bibliographic analysis and review of the material properties, Constr. Build. Mater. 344 (2022) 128143, https://doi.org/10.1016/j.conbuildmat.2022.128143.
- [21] K. Nandhini, J. Karthikeyan, Sustainable and greener concrete production by utilizing waste eggshell powder as cementitious material. A review, Constr. Build. Mater. 335 (2022) 127482, https://doi.org/10.1016/j.conbuildmat.2022.127482.
- [22] N. Sathiparan, Utilization prospects of eggshell powder in sustainable construction material a review, Constr. Build. Mater. 293 (2021) 123465, https://doi.org/10.1016/j.conbiuldmat.2021.123465.
- [23] S. Paruthi, A.H. Khan, A. Kumar, F. Kumar, M.A. Hasan, H.M. Magbool, M.S. Manzar, Sustainable cement replacement using waste eggshells: a review on mechanical properties of eggshell concrete and strength prediction using artificial neural network, Case Stud. Constr. Mater. 18 (2023) e02160, https://doi.org/10.1016/j.cscm.e02160.
- [24] H.M. Hamada, B.A. Tayeh, A. Al-Attar, F.M. Yahada, K. Muthusamy, A.M. Humada, The present state of the use of eggshell powder in concrete: a review, J. Build. Eng. 32 (2020) 101583, https://doi.org/10.1016/j.jobe.2020.101583.
- [25] B.H. Ngayakamo, A. Bello, A.P. Onwualu, Development of eco-friendly fired clay bricks incorporated with granite and eggshell wastes, Environ. Chall. 1 (2020) 100006, https://doi.org/10.1016/j.envc.2020.100006.
- [26] R.A.A. Wahab, M. Mohammad, M. Mazlan, A.N.A. Yaki, N.S.S. Bahari, S.N.A.M. Fadzli, Z.H.B. Zahanis, M.H.M. Zaid, Study on the physical and mechanical properties of low energy consumption fired industrial waste clay bricks from eggshells and rice husk, Mater. Today Proc. 75 (2023) 79–83, https://doi.org/10.1016/j.matpr.2022.10.083.
- [27] J.E.F.M. Ibrahim, O.B. Kotova, S. Sun, E. Kurovics, M. TihTih, L.A. Gömze, Preparation of innovative eco-efficient composite bricks based on zeolite-poor rock and Hen's eggshell, J. Build. Eng. 45 (2022) 103491, https://doi.org/10.1016/j.jobe.2021.103491.
- [28] N. Tangboriboon, S. Moonsri, A. Netthip, W. Sangwan, A. Sirivat, Enhancing physical-thermal-mechanical properties of fired clay bricks by eggshell as a bio-filler and flux, Sci. Sinter. 51 (2019) 1–13, https://doi.org/10.2298/SOS1901001T.
- [29] W. Soliman, Y.M.Z. Ahmed, A. Ghitas, A.H. El Shater, M.A. Shahat, Green building development utilizing modified fired clay bricks and eggshell waste, Sci. Rep. 15 (2025) 3367, https://doi.org/10.1038/s41598-025-87435-4.
- [30] G. Cultrone, C. Rodriguez Navarro, E. Sebastián, O. Cazalla, M.J. de la Torre, Carbonate and silicate phase reactions during ceramic firing, Eur. J. Mineral 13 (2001) 621–634, https://doi.org/10.1127/0935-1221/2001/0013-0621.
- [31] M.J. Trinidade, M.I. Dias, J. Coroado, F. Rocha, Mineralogical transformations of calcareous rich clays with firing: a comparative study between calcite and dolomite rich clays from Algarve, Portugal, Appl. Clay Sci. 42 (2009) 345–355, https://doi.org/10.1016/j.clay.2008.02.008.
- [32] M. Fregenal-Martínez, N. Nieves Meléndez, M.B. Muñoz-García, J. Elez, R. de la Horra, The stratigraphic record of the Late Jurassic-Early Cretaceous rifting in the Alto Tajo-Serranía de Cuenca region (Iberian Ranges, Spain): genetic and structural evidences for a revision and a new lithostratigraphic proposal, Rev. Soc. Geol. Esp. 30 (2017) 113–142.
- [33] B. Bauluz, A. Yuste, M.J. Mayayo, J.I. Canudo, Early kaolinization of detrital Weald facies in the Galve Sub-basin (Central Iberian Chain, north-east Spain) and its relationship to palaeoclimate, Cretac. Res. 50 (2014) 214–227, https://doi.org/10.1016/j.cretres.2014.03.014.
- [34] E. Laita, B. Bauluz, M. Aurell, B. Badenas, J.I. Canudo, A. Yuste, A change from warm/humid to cold/dry climate conditions recorded in lower Barremian clay-dominated continental successions from the SE Iberian Chain (NE Spain), Sediment. Geol. 403 (2020) 105673, https://doi.org/10.1016/j.sedgeo.2020.105673.
- [35] F. Andreola, L. Barbieri, I. Lancellotti, P. Pozzi, Recycling industrial waste in brick manufacture. Part 1, Mater. Construcción 55 (2005) 5–16, https://doi.org/10.3989/mc.2005.v55.i280.202.
- [36] W.D. Kingery, Introduction to Ceramics, John Wiley & Sons, Inc., New York, 1960.
- [37] R.T. Laird, M. Worcester, The inhibiting of lime blowing, Trans. Br. Ceram. Soc. 55 (1956) 545-563.
- [38] UNE-EN 13755, Natural stone test methods, Determination of Water Absorption at Atmospheric Pressure, AENOR, Madrid, Spain, 2008.
- [39] NORMAL 29/88, Misura dell'indice di asciugamento (drying index), ICR-CNR, Rome, Italy, 1988.
- [40] G. Cultrone, M.J. de la Torre, E. Sebastián, O. Cazalla, Evaluación de la durabilidad de ladrillos mediante técnicas destructivas (TD) y no-destructivas (TND), Mater. Construcción 53 (2003) 41–59, https://doi.org/10.3989/mc.2003.v53.i269.267.
- [41] RILEM TC25-PEM, Recommended test to measure the deterioration of stone and to assess the differences of treatment methods, Mater. Struct. 13 (1980) 175–253.
- [42] ASTM D2845, Standard Test Method for Laboratory Determination of Pulse Velocities and Ultrasonic Elastic Constant of Rock, American Society for Testing and Materials, USA, 2005.
- [43] UNE-EN 15886, Conservation of cultural property. Test methods. Colour Measurement of Surfaces, AENOR, Madrid, Spain, 2011.
- [44] UNE-EN 12370, Natural stone test methods, Determination of Resistance to Salt Crystallization, AENOR, Madrid, Spain, 2020.
- [45] L.N. Warr, Recommended abbreviation for the names of clay minerals and associated phases, Clay Miner. 55 (2020) 261–264, https://doi.org/10.1180/clm.2020.30.
- [46] P. Ptáčec, F. Šoukal, T. Opravil, J. Havlika, J. Brandštetr, The kinetic analysis of the thermal decomposition of kaolinite by DTG technique, Powder Technol. 208 (2011) 20–25, https://doi.org/10.1016/j.powtec.2010.11.035.
- [47] G. Cultrone, F.J. Carrillo Rosua, Growth of metastable phases during brick firing: mineralogical and microtextural changes induced by the composition of the raw material and the presence of additives, Appl. Clay Sci. 185 (2020) 105419, https://doi.org/10.1016/j.clay.2019.105419.
- [48] C. Rodriguez Navarro, G. Cultrone, A. Sanchez Navas, E. Sebastian, TEM study of mullite growth after muscovite breakdown, Am. Mineral. 88 (2003) 713–724, https://doi.org/10.2138/am-2003-5-601.
- [49] R. Grapes, Pyrometamorphism, Springer, Berlin, 2006.
- [50] Y. Maniatis, A. Simopoulos, A. Kostikas, Moessbauer study of the effect of calcium content on iron oxide transformations in fired clays, J. Am. Ceram. Soc. 64 (1981) 263–269, https://doi.org/10.1111/j.1151-2916.1981.tb09599.x.
- [51] C. Rodriguez Navarro, E. Ruiz Agudo, A. Luque, A.B. Rodriguez Navarro, M. Ortega Huertas, Thermal decomposition of calcite: mechanisms of formation and textural evolution of CaO nanocrystals, Am. Mineral. 94 (2009) 578–593, https://doi.org/10.2138/am.2009.3021.
- [52] F. García Labiano, A. Abad, L.F. de Diego, P. Gayán, J. Adánez, Calcination of calcium-based sorbents at pressure in a broad range of CO₂ concentrations, Chem. Eng. Sci. 57 (2002) 2381–2393, https://doi.org/10.1016/S00009-2509(02)00137-9.
- [53] E.M. Pérez Monserrat, L. Maritan, G. Cultrone, Firing and post-firing dynamics of Mg- and Ca-rich bricks used in the built heritage of the city of Padua (northeastern Italy), Eur. J. Mineral 34 (2022) 301–319, https://doi.org/10.5194/ejm-34-301-2022.
- [54] K. Traoré, T.S. Kabré, P. Blanchart, Gehlenite and anorthite crystallisation from kaolinite and calcite mix, Ceram. Int. 29 (2003) 377–383, https://doi.org/ 10.1016/S0272-8842(02)00148-7.
- [55] D.L. Whitney, B.W. Evans, Abbreviations for names of rock-forming minerals, Am. Mineral. 95 (2010) 185–187, https://doi.org/10.2138/am.2010.3371.
- [56] M.N. Rahaman, Ceramic Processing and Sintering, second ed., Taylor & Francis Group, 2017.
- [57] Y. Tang, L. Yuan, J. Xue, C. Duan, Experimental study on fracturing coal seams using CaO demolition materials to improve permeability, J. Sustain. Min. 16 (2017) 47–54, https://doi.org/10.1016/j.jsm.2017.07.002.
- [58] L.C. Jain, R. Gopal, S.K. Jain, Lime blowing in bricks, Batiment Int. Build. Res. Practice 4 (1976) 48, https://doi.org/10.1080/09613217608550450.
- [59] G. Cultrone, E. Sebastián, K. Elert, M.J. de la Torre, O. Cazalla, C. Rodríguez Navarro, Influence of mineralogy and firing temperature on porosity of bricks, J. Eur. Ceram. Soc. 24 (2004) 547–564, https://doi.org/10.1016/S0955-2219(03)00249-8.
- [60] G.W. Scherer, Theory of drying, J. Am. Ceram. Soc. 73 (1999) 3–14, https://doi.org/10.1111/j.1151-2916.1990.tb05082.x.
- [61] D. Benavente, L. Linares Fernández, G. Cultrone, E. Sebastián, Influence of the microstructure on the resistance to salt crystallization damage in brick, Mater. Struct. 39 (2006) 105–113, https://doi.org/10.1617/s11527-005-9037-0.
- [62] A. De Bonis, G. Cultrone, C. Grifa, A. Langella, V. Morra, Clays from the Bay of Naples (Italy): new insight on ancient and traditional ceramics, J. Eur. Ceram. Soc. 34 (2014) 3229–3244, https://doi.org/10.1016/j.jeurceramimsoc.2014.04.014.
- [63] ISO 13006, Ceramic Tiles. Definitions, Classification, Characteristics and Marking, Geneva, Switzerland, 2018.

- [64] M. Tite, Y. Maniatis, Examination of ancient pottery using the scanning electron microscope, Nature 257 (1975) 122–123.
- [65] F. Singer, S.S. Singer, Industrial Ceramics, Chapman & Hall, London, 1963.
- [66] ICOMOS-ISCS, Illustrated glossary on stone deterioration patterns, in: V. Vergès Belmin (Ed.), Monuments and Sites XV, France, 2008.
- [67] L. Crespo López, A. Martínez Ramirez, E. Sebastián, G. Cultrone, Pomace from the wine industry as an additive in the production of traditional sustainable
- lightweight eco-bricks, Appl. Clay Sci. 243 (2023) 107084, https://doi.org/10.1016/j.clay.2023.107084.

 [68] L. Crespo López, C. Coletti, A. Arizzi, G. Cultrone, Effects of using tea waste as an additive in the production of solid bricks in terms of their porosity, thermal conductivity, strength and durability, Sustain. Mater. Technol. 39 (2024) e00859, https://doi.org/10.1016/j.susmat.2024.e00859
- [69] C. Coletti, L. Maritan, G. Cultrone, C. Mazzoli, Use of industrial ceramic sludge in brick production: effects on aesthetic quality and physical properties, Constr. Build. Mater. 124 (2016) 219–227, https://doi.org/10.1016/jconbuildmat.2016.07.096.